PAPER

Check for updates

(±)-Applanatumines B–D: novel dimeric meroterpenoids from *Ganoderma applanatum* as inhibitors of JAK3†

Qi Luo,[ab] Zhen Wang,[c] Jin-Feng Luo,[c] Zheng-Chao Tu[*c] and Yong-Xian Cheng [ID] [*ad]

Applanatumines B–D (1–3), three pairs of dimeric meroterpenoid enantiomers featuring the presence of a 6-oxo-4,4a,5,5a,6,8,8a,8b-octahydrofuro[3′,4′:4,5]cyclopenta[1,2-*b*]pyran-3-carbaldehyde structure core, were isolated from the fruiting bodies of *Ganoderma applanatum*. Their structures and absolute configurations were assigned by using spectroscopic methods and ECD calculations. Biological evaluation found that all the compounds are JAK3 inhibitors. In addition, the enantiomers of **1** are active towards DDR1 with IC_{50} values of 8.2 ± 0.8 μM and 6.9 ± 0.8 μM. Finally, a plausible biogenic pathway for compounds **1–3** was proposed.

1. Introduction

Ganoderma (Ganodermataceae) are mainly spread over tropical and subtropical regions.[1] Of hundreds of fungal species in this genus, many are of great medicinal values and are even called cure-all medicine, implying their wide range of therapeutic applications.[2] Despite the medicinal importance of *Ganoderma*, chemical investigation on this genus has mainly focused on triterpenoids and polysaccharides,[3,4] which could only in part unveil the scientific connotation of *Ganoderma*-based traditional medicine; the chemical and biological profiles of *Ganoderma* fungi need further exploration. Oxidative stress and inflammation are implicated in multiple diseases; with this context, we have characterized a series of structurally novel meroterpenoids from *Ganoderma* with antioxidant or anti-inflammatory properties; a subsequent investigation revealed that they are either Nrf2 activators or TGF-β/Smad3 inhibitors,[5–7] showing that meroterpenoids in *Gnoderma* are promising structure templates. Indeed, lingzhiols have attracted great attention since they were reported in 2013.[8–14]

[a]State Key Laboratory of Phytochemistry and Plant Resources in West China, Kunming Institute of Botany, Kunming 650204, People's Republic of China. E-mail: yxcheng@mail.kib.ac.cn

[b]University of Chinese Academy of Sciences, Yuquan Road 19, Beijing 100049, People's Republic of China

[c]Drug Discovery Pipeline, Guangdong Provincial Key Laboratory of Biocomputing, Guangzhou Institutes of Biomedicine and Health, Guangzhou 510530, People's Republic of China. E-mail: tu_zhengchao@gibh.ac.cn

[d]School of Pharmaceutical Sciences, Shenzhen University Health Sciences Center, Shenzhen 518060, People's Republic of China

† Electronic supplementary information (ESI) available: ECD calculation methods, 1D, 2D, HRESIMS spectra, and HPLC chromatograms. See DOI: 10.1039/c7ra04862a
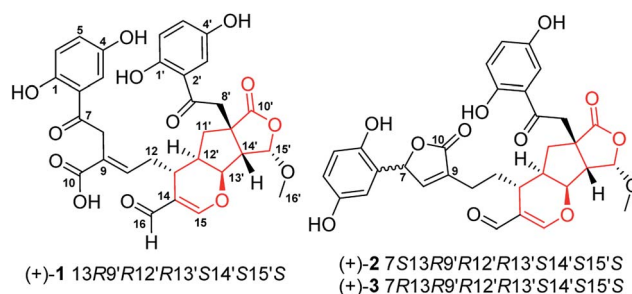
Fig. 1 The structures of novel dimeric meroterpenoids 1–3.

Janus kinase 3 (JAK3), discoidin domain receptor 1 (DDR1), histone deacetylase 1 (HDAC1) and bromodomain-containing protein 4 (BRD4) have emerged as promising drug targets for a number of diseases such as cancer, fibrosis, and rheumatoid arthritis.[15–17] In consideration of wide applications of *Ganoderma* species, it is therefore necessary to examine whether substances in this genus possess inhibitory activities towards the above established targets. With this motivation, we have conducted a chemical investigation focusing meroterpenoids in *Ganoderma applanatum* and reported structurally novel applanatumine A.[6,7,18] In a follow up study on this fungus, applanatumines B–D (**1–3**) (Fig. 1), three pairs of novel dimeric meroterpenoid enantiomers, were characterized and their biological activities against JAK3, DDR1, HDAC1, and BRD4 were evaluated.

2. Results and discussion

2.1. Structure elucidation

The EtOH extract of *G. applanatum* was suspended in H_2O and partitioned with EtOAc. A combination of chromatography of an

EtOAc soluble fraction afforded 3 racemic meroterpenoid dimers.

(±)-Compound **1** was obtained as yellow gum with the molecular formula of $C_{32}H_{30}O_{13}$ determined by analysis of its HRESIMS (m/z 621.1605 [M − H]$^-$, calcd for $C_{32}H_{29}O_{13}$, 621.1614), ^{13}C NMR and DEPT data, indicating 18 degrees of unsaturation. The ^1H NMR spectrum (Table 1) contains two typical ABX proton coupling systems [δ_H 7.36 (1H, d, $J = 2.8$ Hz, H-3), 7.01 (1H, dd, $J = 8.8, 2.8$ Hz, H-5) and 6.79 (1H, d, $J = 8.8$ Hz, H-6)] and [δ_H 7.18 (1H, d, $J = 2.8$ Hz, H-3′), 7.01 (1H, dd, $J = 8.8, 2.8$ Hz, H-5′) and 6.81 (1H, d, $J = 8.8$ Hz, H-6′)], suggesting the presence of two 1,2,4-trisubstituted benzene substructures.

The ^{13}C NMR and DEPT spectra of **1** (Table 1) contain 32 resonances attributable to a methyl (oxygenated), four methylenes, fourteen methines (eight olefinics, an aldehyde group), thirteen quaternary carbons (eight sp^2, two ketones, two carboxylic carbonyls, and an aliphatic carbon). The partial signals occur as pairs, suggesting that **1** might be a meroterpenoid dimer consisting of parts A (black drawing) and B

(blue drawing) (Fig. 2). The ABX coupling pattern, the chemical shifts of C-1 (δ_C 156.4) and C-4 (δ_C 150.7), and HMBC correlations of H-3/C-7, H-11/C-8 (δ_C 37.3), and ROESY correlation of H-3/H-8 indicate the substructure of C-1–C-10. The HMBC
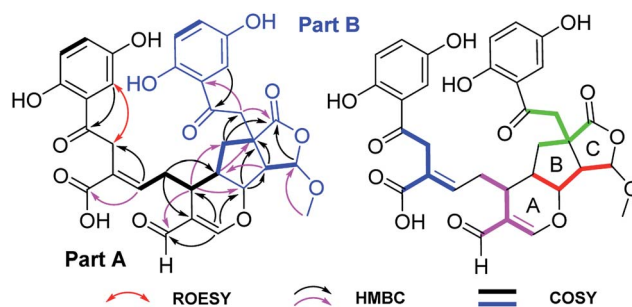

Fig. 2 Key ^1H–^1H COSY and HMBC correlations of **1**, and ROESY correlation of H-3/H-8; blue, pink, red, and green in **1** represent four independent isoprenyl moieties.

Table 1 The ^1H (600 MHz) and ^{13}C NMR (150 MHz) data of **1–3** (δ in ppm) in methanol-d_4

No.	1 δ_H	1 δ_C	2 δ_H	2 δ_C	3 δ_H	3 δ_C
1		156.4		149.0		149.1
2		120.8		123.4		123.3
3	7.36 d (2.8)	115.8	6.49 d (2.6)	113.4	6.50 d (2.8)	113.6
4		150.7		151.5		151.4
5	7.01 dd (8.8, 2.8)	125.7	6.61 dd (8.6, 2.6)	117.3	6.62 dd (8.6, 2.8)	117.3
6	6.79 d (8.8)	119.6	6.68 d (8.6)	117.3	6.69 d (8.6)	117.4
7		204.7	6.26 br s	79.9	6.26 br s	80.0
8	4.05 s	37.3^b	7.47 br s	151.1	7.47 br s	151.0
9		128.4^b		133.2		133.3
10		172.4^b		176.6		176.7
11	7.03 t (4.0)	142.2^b	2.37 m	23.6	2.38 m	23.5
12	Ha 2.53 m / Hb 2.30 m	35.0	Ha 1.86 m / Hb 1.64 m	34.5	Ha 1.86 m / Hb 1.63 m	34.8
13	2.65 dd (8.5, 4.7)	30.0	2.52 dd (8.5, 4.7)	29.3	2.53 dd (8.5, 4.7)	29.2
14		120.5		121.4		121.3
15	7.51 s	166.5	7.49 s	166.3	7.48 s	166.4
16	9.22 s	193.3	9.22 s	193.4	9.23 s	193.4
1′		156.4		156.4		156.4
2′		120.2		120.1		120.1
3′	7.18 d (2.8)	115.3	7.18 d (2.6)	115.3	7.18 d (2.6)	115.3
4′		150.9		150.8		150.8
5′	7.01 dd (8.8, 2.8)	126.5	7.03 dd (8.8, 2.6)	126.5	7.02 dd (8.8, 2.6)	126.5
6′	6.81 d (8.8)	119.9	6.80 d (8.8)	119.9	6.80 d (8.8)	119.9
7′		204.7		204.7		204.7
8′	Ha 3.79 d (19.0) / Hb 3.43 d (19.0)	48.3	Ha 3.78 d (19.0) / Hb 3.42 d (19.0)	48.5	Ha 3.79 d (19.0) / Hb 3.42 d (19.0)	48.5
9′		53.0		53.0		53.0
10′		181.8		181.9		181.9
11′	Ha 2.24 dd (13.5, 7.2) / Hb 1.63 t-like (13.5)	41.3	Ha 2.20 dd (13.4, 7.3) / Hb 1.61 t (13.4)	41.0	Ha 2.22 dd (13.4, 7.3) / Hb 1.61 t (13.4)	41.0
12′	2.37 m	40.1	2.46 m	39.9	2.46 m	39.9
13′	4.85^a	81.7	4.85^a	81.6	4.85^a	81.6
14′	3.21 d (7.6)	55.1	3.21 d (7.5)	54.9	3.21 d (7.6)	54.9
15′	5.94 d (7.6)	105.7	5.94 d (7.5)	105.6	5.94 d (7.6)	105.6
16′	3.63 s	59.0	3.64 s	58.8	3.64 s	58.9

^{a} Overlapped signals by measured solvent. ^{b} Signals were assigned by HMBC experiment.

correlations of H-15 (δ_H 7.51)/C-13, C-14, C-16 (δ_C 193.3), C-13′ (δ_C 81.7); H-13/C-13′; and H-16 (δ_H 9.22)/C-13, C-14, C-15 (δ_C 166.5), in combination with a ^{1}H–^{1}H COSY correlation of H-13/H-12′ (Fig. 2) indicate the existence of ring A with an aldehyde group attached to C-14. Further, the HMBC correlations of H-11/C-8, C-10, and COSY correlation of H-12/H-13 were observed, which reveals the presence of part A as shown. In addition to the signals for part A, the residual signals resemble those of lingzhilactone C, a meroterpenoid previously isolated from *G. lingzhi*.[5] This conclusion gains supports from 2D NMR data, which show important interactions such as HMBC correlations of H-13′/C-9′, C-11′; H-14′/C-9′, C-10′, C-12′, C-13′, C-15′; H-15′/C-10′ and COSY correlations of H-9′/H-11′/H-12′ and H-14′/H-15′, indicating the ring systems in part B. Finally, parts A and B are connected *via* C-12′–C-13′ supported by the observed ^{1}H–^{1}H COSY correlations of H-13/H-12′/H-11′ as well as above mentioned H-15/C-13′. As a result, the planar structure of **1** was determined.

The relative configuration of **1** was assigned by a ROESY spectrum (Fig. 3), which shows correlations of H-12/H-12′, H-13′, indicating the relative configuration of ring A. The ROESY correlation of H-8′/H-14′ suggests that these two protons are at the same side of ring B. Further, the observed ROESY correlations between H-13/Ha-11′, Hb-11′ and H-8′, H-14′/Hb-11′ indicate the stereo relationship between rings A and B. As for the relative configuration at C-15′, the observed ROESY correlation of 15′-OMe/H-12′ and weak correlation H-15′/Ha-8′ evidently suggests that the orientation of H-15′. Therefore, the relative configurations at chiral centers of rings B and C were determined. Besides, there is one double bond $\Delta^{9(11)}$ at the side chain of part A, whose geometry was assigned as *E*-form based on the observed ROESY correlation of H-8/Hb-12.
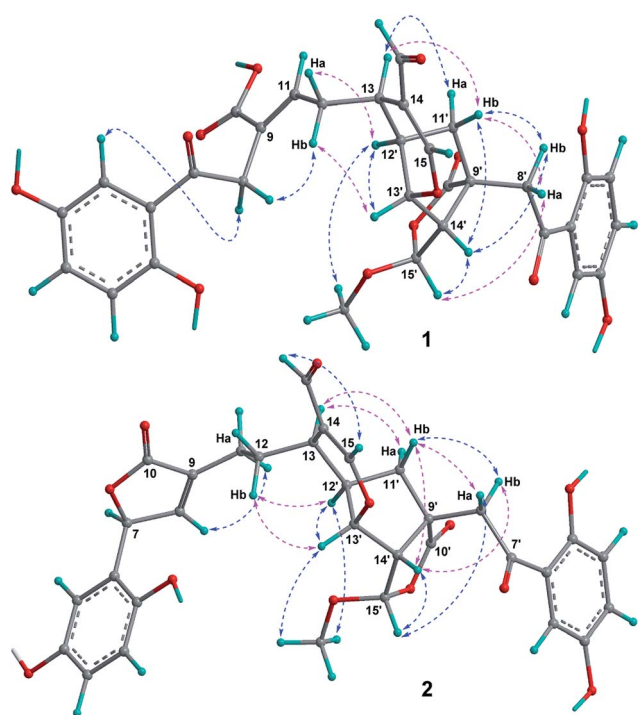
(±)-**1** was isolated as a racemate (Fig. S25, ESI†), which further was separated by chiral-phase HPLC. In order to determine the absolute configuration of (+)-**1** and (−)-**1**, the electronic circular dichroism (ECD) calculations were carried out. It was found that the ECD spectrum of (13*R*,9′*R*,12′*R*,13′*S*,14′*S*,15′*S*)-**1** agrees well with the experimental one of (+)-**1**, leading to the assignment of the absolute configuration at the stereogenic centers (Fig. 4). Consequently, the structures of (+)-**1** and (−)-**1** were finally assigned and named (±)-applanatumine B.

Simultaneously, a portion was purified by a semipreparative HPLC (Fig. S24, ESI†) to yield **2** (Rt = 17.5 min) and **3** (Rt = 19.8 min), and they are both racemic mixtures (Fig. S26 and S27, ESI†). Compounds **2** and **3** possess the same planar structure by analysis of their HRESIMS, 1D and 2D NMR data. Furthermore, a detailed interpretation of their 1D and 2D data (**1**–**3**), the only difference is that the existence of a five-membered lactone in **2** or **3**, which was confirmed by the HMBC correlations of H-7/C-8 (δ_C 151.1), C-9 (δ_C 133.2), C-10 (δ_C 176.6), and H-8/C-7 (δ_C 79.9), C-9, C-10 (Fig. 5). The relative configuration of **2** was assigned by a ROESY spectrum which shows correlations of H-12′, H-13′/Hb-12, suggesting the relative configurations at C-13, C-12′, and C-13′. Likewise, the correlations of H-14′/Hb-8′, H-15′/Ha-8′, and 15′-OMe/H-12′, H-13′ (Fig. 3) reveal the relative configurations at C-9′, C-14′, and C-15′. As for the stereochemistry at C-7, it makes sense only to determine its absolute configuration.

Careful analysis of ROESY data of **3** reveals that compounds **3** and **2** bear the same relative configuration at C-13, C-9′, C-12′, C-13′, C-14′, and C-15′. Likewise, the assignment of stereochemistry at C-7 of **3** is challengeable. To clarify the absolute configuration at C-7, racemic **2** or **3** was submitted to chiral-phase HPLC to afford their respective enantiomers. By comparing the experimental spectra of **2** and **3**, it was fortunately found that their experimental CD spectra have obvious difference at 197 nm and 207 nm [$\Delta\varepsilon_{197}$ −16.50, $\Delta\varepsilon_{207}$ +3.91 for (+)-**2**, no cotton effective for (+)-**3**], which makes it possible to use computational methods to solve the configuration at C-7. An effort of computation found that the calculated weighted ECD spectra of (7*S*,13*R*,9′*R*,12′*R*,13′*S*,14′*S*,15′*S*)-**2** agree well with that of (+)-**2** (Fig. 6 and 7). Hence, the absolute configurations of (+)-**2** and (−)-**2** were unambiguously assigned. In the same manner as that of **2**, the absolute configurations of (+)-**3** and (−)-**3** were
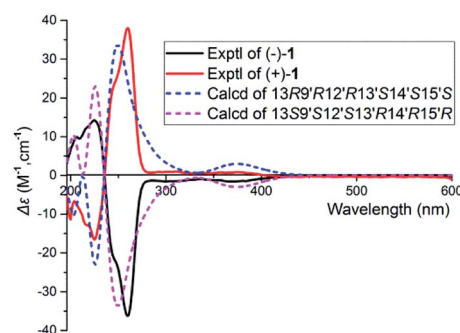

Fig. 3   Key ROESY correlations of **1** and **2**.

Fig. 4   Experimental and calculated ECD spectra of **1** at the B3LYP/6-311G(d,p) level in MeOH, σ = 0.3 eV.
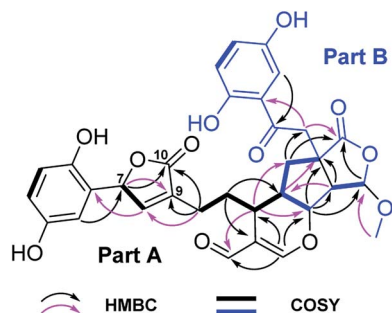
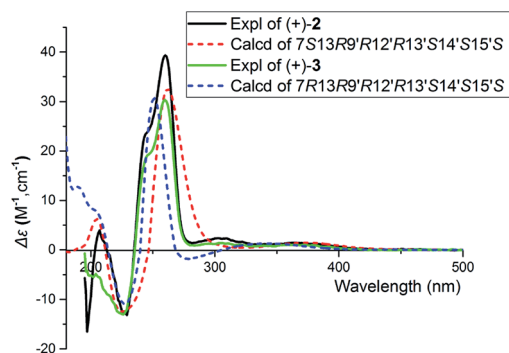Fig. 5 Key ^{1}H–^{1}H COSY and HMBC correlations of **2** or **3**.

Fig. 6 The calculated ECD spectra and experimental spectra of (+)-**2** and (+)-**3** at the B3LYP/6-311G(d,p) level in MeOH, σ = 0.3 eV.
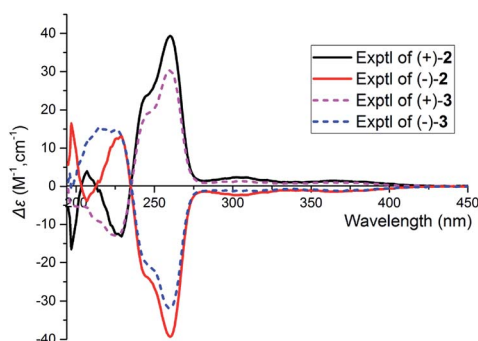

Fig. 7 The experimental spectra of (+)-**2**, (−)-**2**, and (+)-**3**, (−)-**3** in MeOH.

respectively assigned as 7R,13R,9′R,12′R,13′S,14′S,15′S and 7S,13S,9′S,12′S,13′R,14′R,15′R (Fig. 6 and 7). Obviously, (+)-**3** is a 7-epimer of (+)-**2**.

Compounds **1–3** are novel meroterpenoid dimers. The formation of rings A–C leads to the presence of six continuous chiral centers in the structure, providing great challenge for synthetic chemistry. To aid total synthesis of this class of meroterpenoids, a plausible biosynthetic pathway was proposed. Compounds **1–3** are derived from the hybridization of shikimic acid pathway and mevalonic acid pathway[18] (Scheme 1). First, two key intermediates A and B could be synthesized from 4-hydroxybenzonic acid (4HB)[18] and isoprenyl moieties under geranyltransferase[19] and VibMO1 (a monooxygenase).[20] The

intermediate A is further oxidized to give B. The monomer B could be cyclized via nucleophilic addition to generate C and F. In addition, the monomer E is formed by oxidation reaction and decarboxylization of C. Hence, **2** and **3** are further formed by a Diels–Alder reaction between E and F. Finally, the monomer G is formed by oxidation reaction and 1,3-hydrogen migration of B, and the ring A in **1** is formed via a Diels–Alder reaction between E and G.

2.2. Biological evaluation

To explore the biological activities of meroterpenoids in the genus *Ganoderma*, all the isolates were tested for their inhibitory activities towards JAK3, DDR1, HDAC1, and BRD4 (Table 2). It was found that almost all the compounds are active in these assays. Of particular, JAK3 kinase is sensitive for compounds **1–3** with IC_{50} values less than 10 μM. In addition, the enantiomers of **1** are active towards DDR1 with IC_{50} values of 8.2 ± 0.8 μM and 6.9 ± 0.8 μM, respectively. It is worthwhile that DDR1, HDAC1, and BRD4 are all promising epigenetic drug targets for a number of diseases. Despite the less potency of these compounds than synthetic agents, the present findings suggest that these natural meroterpenoids could be considered as a new scaffold for the development of more potent epigenetic agents.

3. Experimental section

3.1. General procedure

Optical rotations were recorded on a Jasco P-1020. UV spectra were collected on a Shimadzu UV2401PC. CD spectra were measured on an Agilent applied photophysics. NMR spectra were determined on a Brucker AV 600 MHz. ESIMS and HRE-SIMS were measured on an Agilent UPLC/Q-TOF. RP-18 (40–60 μm, Daiso Co., Japan), MCI gel CHP 20P (75–150 μm, Tokyo, Japan), and Sephadex LH-20 (Amersham Biosciences, Sweden). Semipreparative HPLC was carried out using an Agilent 1200 liquid chromatograph and a LC-3000 high liquid chromatograph that made in China, the columns used were a 250 mm × 9.4 mm i.d., 5 μm, Zorbax SB-C$_{18}$ and a 250 mm × 10 mm, i.d., 5 μm, Daicel Chiralpak (IC), flow rate: 2.5 mL min^{-1}.

3.2. Fungal material

The fruiting bodies of *G. applanatum* were purchased from Tong-kang Pharmaceutical Co. Ltd. in Guangzhou Province, People's Republic of China, in September 2013. The material was identified by Prof. Zhu-Liang Yang at Kunming Institute of Botany, Chinese Academy of Sciences, and a voucher specimen (CHYX-0590) was deposited at the State Key Laboratory of Photochemistry and Plant Resources in West China, Kunming Institute of Botany, Chinese Academy of Sciences, People's Republic of China.

3.3. Extraction and isolation

Powdered fruiting bodies of *G. applanatum* (30 kg) were extracted by refluxing with 80% EtOH (3 × 120 L × 2 h) and concentrated under reduced pressure to give a crude extract, which was suspended in water followed by extraction with EtOAc to afford an EtOAc soluble extract. The EtOAc extract (0.9
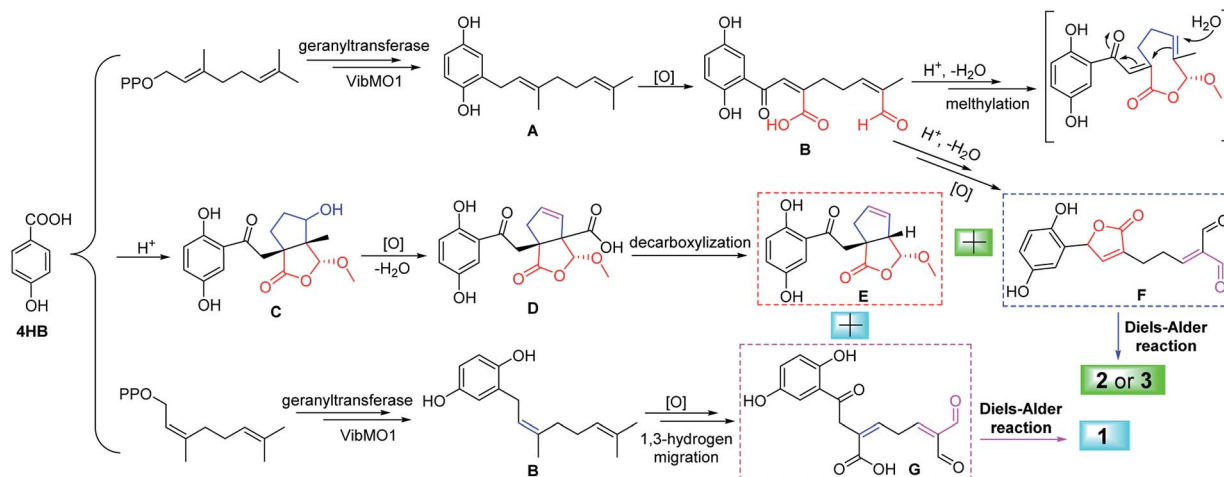
Scheme 1 Proposed biogenetic pathway for compounds **1–3**.

kg) was divided into seven parts (Fr.1–Fr.7), by using a MCI gel CHP 20P column eluted with aqueous MeOH (20–100%). Fr.5 (32.0 g) was separated by MCI gel CHP 20P eluted with gradient aqueous MeOH (40–80%) to yield six fractions (Fr.5.1–Fr.5.6). Of which, Fr.5.5 (7.3 g) was further divided into six portions (Fr.5.5.1–Fr.5.5.6) by RP-18 with aqueous MeOH (60–80%). Fr.5.5.6 (1.1 g) was separated by Sephadex LH-20 (MeOH) followed by semipreparative HPLC (MeOH–H_2O, 59%) to yield **1** (1.2 mg, Rt = 21.3 min), **2** (9.0 mg, Rt = 17.5 min), and **3** (12.0 mg, Rt = 19.8 min). Compounds **1–3** were isolated as racemate, which were further purified by chiral-phase HPLC on Daicel Chiralpak IC (flow rate: 2.5 mL min^{-1}) to afford enantiomers [(−)-**1** (0.5 mg, Rt = 17.5 min), (+)-**1** (0.4 mg, Rt = 19.7 min), n-hexane–EtOH–HCOOH, 80 : 20 : 0.01%; (+)-**2** (4.2 mg, Rt = 21.8 min), (−)-**2** (4.3 mg, Rt = 25.9 min), n-hexane–EtOH, 80 : 20; and [(+)-**3** (5.6 mg, Rt = 20.4 min), (−)-**3** (5.7 mg, Rt = 23.0 min), n-hexane–EtOH, 80 : 20].

3.4. Spectral data of 1–3

Applanatumin B (**1**): yellow gum, UV (MeOH) λ_{max} (log ε): 373 (3.51), 253 (3.91), 226 (4.00) nm; $\{[\alpha]_D^{24}$ +163.8 (c 0.07, MeOH), CD (MeOH) $\Delta\varepsilon_{225}$ −17.08, $\Delta\varepsilon_{260}$ +38.26, for (+)-**1**; $[\alpha]_D^{24}$ −166.0 (c 0.05, MeOH), CD (MeOH) $\Delta\varepsilon_{224}$ +14.32, $\Delta\varepsilon_{260}$ −36.36, for (−)-**1**}; ESIMS: m/z 621 [M − H]$^-$; HRESIMS: m/z 621.1605 [M − H]$^-$ (calcd for $C_{32}H_{29}O_{13}$, 621.1614); ^{1}H and ^{13}C NMR data, see Table 1.

Applanatumin C (**2**): yellow gum, UV (MeOH) λ_{max} (log ε): 370 (3.53), 250 (4.17), 221 (4.25) nm; $\{[\alpha]_D^{24}$ +159.3 (c 0.18, MeOH), CD (MeOH) $\Delta\varepsilon_{197}$ −16.50, $\Delta\varepsilon_{207}$ +3.91, $\Delta\varepsilon_{229}$ −13.10, $\Delta\varepsilon_{260}$ +39.30, for (+)-**2**; $[\alpha]_D^{24}$ −199.2 (c 0.16, MeOH), CD (MeOH) $\Delta\varepsilon_{197}$ +16.50, $\Delta\varepsilon_{208}$ −3.91, $\Delta\varepsilon_{229}$ +11.28, $\Delta\varepsilon_{260}$ −33.67, for (−)-**2**}; ESIMS: m/z 605 [M − H]$^-$; HRESIMS: m/z 719.1590 [M + CF$_3$COO]$^-$ (calcd for $C_{34}H_{30}O_{14}F_3$, 719.1593); ^{1}H and ^{13}C NMR data, see Table 1.

Applanatumin D (**3**): yellow gum, UV (MeOH) λ_{max} (log ε): 368 (3.62), 251 (4.24), 227 (4.30) nm; $\{[\alpha]_D^{24}$ +208.9 (c 0.30, MeOH), CD (MeOH) $\Delta\varepsilon_{226}$ −13.03, $\Delta\varepsilon_{259}$ +30.31, for (+)-**3**; $[\alpha]_D^{24}$ −229.6 (c 0.33, MeOH), CD (MeOH) $\Delta\varepsilon_{225}$ +14.97, $\Delta\varepsilon_{260}$ −31.95, for (−)-**3**}; ESIMS: m/z 605 [M − H]$^-$; HRESIMS: m/z 719.1587 [M + CF$_3$COO]$^-$ (calcd for $C_{34}H_{30}O_{14}F_3$, 719.1593); ^{1}H and ^{13}C NMR data, see Table 1.

3.5. ECD calculation

The CONFLEX 7 searches based on molecular mechanics with MMFF94S force fields were performed for model compounds of

Table 2 Activities of compounds **1–3**^{a}

Compounds	IC$_{50}$ (μM)			
	JAK3	DDR1	HDAC1	BRD4
(+)-**1**	1.8 ± 0.9	8.2 ± 0.8	212.0 ± 53.2	38.9 ± 5.3
(−)-**1**	2.0 ± 0.9	6.9 ± 0.8	268.0 ± 0.2	46.5 ± 16.1
(+)-**2**	0.8 ± 0.7	~10.0	19.1 ± 10.4	39.5 ± 5.9
(−)-**2**	6.1 ± 1.0	NA	45.4 ± 9.2	68.5 ± 19.4
(+)-**3**	3.8 ± 1.0	NA	46.6 ± 20.1	19.9 ± 8.0
(−)-**3**	3.8 ± 0.3	NA	36.1 ± 1.5	27.8 ± 1.5
Staurosporine	(0.3 ± 0.01) × 10^{-3}			
Dasatinib		(13.2 ± 0.1) × 10^{-3}		
JQ-1			(2.4 ± 0.6) × 10^{-3}	0.1 ± 0.06

^{a} NA: no activity.
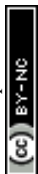
1–**3**, respectively. The predominant conformers were optimized and calculated by DFT calculation at B3LYP/6-311G(d,p) level with the PCM in MeOH. Under the circumstances, all the above calculations were carried out with the Gaussian 09 package of programs.[21] For comparison of the calculated curves and experimental CD spectra, the program SpecDis[22] was used.

3.6. *In vitro* JAK3 kinase inhibitory activity assay

The inhibitory activity of compounds **1**–**3** against JAK3 kinase was performed using the FRET-based Z'-Lyte assay system in line with the manufacturer's instructions (Invitrogen, Carlsbad, USA) and previously described methods.[23] In this study, staurosporine was used as a positive control. The data were analyzed using Graphpad Prism5 (Graphpad Software, Inc).

3.7. *In vitro* DDR1 kinase inhibitory activity assay

Compounds **1**–**3** were evaluated for their inhibitory activity towards DDR1 kinase using a LanthaScreen Eu kinase activity assay technology (Invitrogen, USA) as previously described.[23] In this study, dasatinib was used as a positive control.

3.8. *In vitro* HDAC1 inhibition assay

The purified recombinant human HDAC1 and their corresponding substrates were purchased from BPS Bioscience (BPS Bioscience Inc., USA). The assays were carried out in 384-well format using the BPS fluorescent-based HDAC activity assay according to the manufacturer's protocol (BPS Bioscience Inc., USA). The HDAC reaction mixture was composed of HDAC assay buffer (BPS Bioscience Inc., USA), BSA, serial diluted test compounds, appropriate concentration of HDACs, and 20 μM fluorogenic substrate. The mixture was incubated at 37 °C for 60 min and then stopped by addition of developer containing trypsin and TSA. After 20 min of incubation, fluorescence was detected at the excitation wavelength of 360 nm and the emission wavelength of 460 nm using EnVision multilabel reader (PerkinElmer Inc., USA). JQ-1 was used as the positive control. The analytical software, GraphPad Prism 5.0 (GraphPad Software, Inc., USA) was used to generate IC_{50} value *via* nonlinear regression analysis.

3.9. *In vitro* BRD4 inhibition assay

In vitro inhibitory activity of compounds on BRD4 was carried out in 384-well plates by TR-FRET assay using BRD4 (BD1) TR-FRET Assay Kit (BPS BioScience, San Diego, CA, USA) according to the manufacturer's instructions. In brief, 2.5 μL of BRD assay buffer was added 2.5 μL of BET bromodomain ligand and 2.5 μL of BRD4 (BD1) and appropriate serials of diluted compounds, subsequently mixed with GSH Acceptor beads (PerkinElmer #AL109C) and Streptavidin-conjugated donor beads (PE #6760002S). After 1 h room temperature incubation, the plates were measured in EnVision Multilabel Reader (Perkin Elmer, Inc.) using TR-FRET module with excitation 340 nm and emission 665 nm). JQ-1 was used as the positive control.

4. Conclusions

In sum, the present study afforded three unprecedented meroterpenoid dimers from the fruiting bodies of *G. applanatum*. These metabolites were all isolated as racemic mixtures. ECD calculations were successfully used to clarify the absolute configurations of the enantiomers. Meroterpenoids **1**–**3** were found to be JAK3, DDR1, HDAC1, and BRD4 inhibitors with an unprecedented structure type. Of note, their inhibitory activities towards JAK3 and DDR1 are significant, we envision that compounds **1**–**3** might serve as a useful scaffold for the development of more potent therapeutic agents (including epigenetic agents) against these targets associated diseases such as cancer, fibrosis, and rheumatoid arthritis.

Notes and references

1 C. Richter, K. Wittstein, P. M. Kirk and M. Stadler, *Fungal Divers.*, 2015, **71**, 1.

2 R. R. M. Paterson, *Phytochemistry*, 2006, **67**, 1985.

3 K. Wang, L. Bao, W. P. Xiong, K. Ma, J. J. Han, W. Z. Wang, W. B. Yin and H. W. Liu, *J. Nat. Prod.*, 2015, **78**, 1977.

4 I. C. F. R. Ferreira, S. A. Heleno, F. S. Reis, D. J. Stojkovic, M. J. R. P. Queiroz, M. H. Vasconcelos and M. Sokovic, *Phytochemistry*, 2015, **114**, 38.

5 (*a*) Y. M. Yan, J. Ai, Y. N. L. L. Zhou, A. C. K. Chung, R. Li, J. Nie, P. Fang, X. L. Wang, J. Luo, Q. Hu, F. F. Hou and Y. X. Cheng, *Org. Lett.*, 2013, **15**, 5488; (*b*) F. J. Zhou, Y. Nian, Y. M. Yan, Y. Gong, Q. Luo, Y. Zhang, B. Hou, Z. L. Zuo, S. M. Wang, H. H. Jiang, J. Yang and Y. X. Cheng, *Org. Lett.*, 2015, **17**, 3082; (*c*) Q. Luo, L. Tian, L. Di, Y. M. Yan, X. Y. Wei, X. F. Wang and Y. X. Cheng, *Org. Lett.*, 2015, **17**, 1565; (*d*) Q. Luo, X. L. Wang, L. Di, Y. M. Yan, Q. Lu, X. H. Yang, D. B. Hu and Y. X. Cheng, *Tetrahedron*, 2015, **71**, 840; (*e*) Y. M. Yan, X. L. Wang, L. L. Zhou, F. J. Zhou, R. Li, Y. Tian, Z. L. Zuo, P. Fang, A. C. K. Chung, F. F. Hou and Y. X. Cheng, *J. Ethnopharmacol.*, 2015, **176**, 385; (*f*) Q. Luo, Z. L. Yang, Y. M. Yan and Y. X. Cheng, *Org. Lett.*, 2017, **19**, 718.

6 (*a*) Q. Luo, X. H. Yang, Z. L. Yang, Z. C. Tu and Y. X. Cheng, *Tetrahedron*, 2016, **72**, 4564; (*b*) Q. Luo, L. Di, X. H. Yang and Y. X. Cheng, *RSC Adv.*, 2016, **6**, 45963; (*c*) Q. Luo, Z. C. Tu and Y. X. Cheng, *RSC Adv.*, 2017, 7, 3413.

7 Q. Luo, X. Y. Wei, J. Yang, J. F. Luo, R. Liang, Z. C. Tu and Y. X. Cheng, *J. Nat. Prod.*, 2017, **80**, 61.

8 R. Long, J. Huang, W. B. Shao, S. Liu, Y. Lan, J. X. Gong and Z. Yang, *Nat. Commun.*, 2014, **5**, 5707.

9 X. Y. Li, X. Y. Liu, X. Z. Jiao, H. G. Yang, Y. Y. Yao and P. Xie, *Org. Lett.*, 2016, **18**, 1944–1946.

10 K. S. Gautam and V. B. Birman, *Org. Lett.*, 2016, **18**, 1499–1501.

11 D. Chen, H. M. Liu, M. M. Li, Y. M. Yan, W. D. Xu, X. N. Li, Y. X. Cheng and H. B. Qin, *Chem. Commun.*, 2015, **51**, 14594–14596.

12 R. Rengarasu and M. E. Maier, *Asian J. Org. Chem.*, 2017, **6**, 108–117.

13 R. A. Hill and A. Sutherland, *Nat. Prod. Rep.*, 2014, **31**, 148–153.

14 Y. Liu, C. J. Zhou, Q. J. Li and H. G. Wang, *Org. Biomol. Chem.*, 2016, **14**, 10362.

15 J. Y. Song, X. Chen, J. Bai, Q. H. Liu, H. Li, J. W. Xie, H. Jing and J. N. Zheng, *Tumor Biol.*, 2016, **37**, 11509.

16 J. Y. Yan, Z. M. Zhang, J. Yang, W. Mitch and Y. L. Wang, *J. Am. Soc. Nephrol.*, 2015, **26**, 3060.

17 N. Ding, N. Hah, R. T. Yu, M. H. Sherman, C. Benner, M. Leblanc, M. X. He, C. Liddle, M. Dowens and R. M. Evans, *Proc. Natl. Acad. Sci. U. S. A.*, 2015, **112**, 15713.

18 Q. Luo, L. Di, W. F. Dai, Q. Lu, Y. M. Yan, Z. L. Yang, R. T. Li and Y. X. Cheng, *Org. Lett.*, 2015, **17**, 1110.

19 R. Boehm, S. Sommer, S. M. Li and L. Heide, *Plant Cell Physiol.*, 2000, **8**, 911.

20 Y. L. Yang, H. Zhou, G. Du, K. N. Feng, T. Feng, X. L. Fu, J. K. Liu and Y. Zeng, *Angew. Chem., Int. Ed.*, 2016, **55**, 5463.

21 M. J. Frisch, G. W. Trucks, H. B. Schlegel, G. E. Scuseria, M. A. Robb, J. R. Cheeseman, G. Scalmani, V. Barone, B. Mennucci, G. A. Petersson, H. Nakatsuji, M. Caricato, X. Li, H. P. Hratchian, A. F. Izmaylov, J. Bloino, G. Zheng, J. L. Sonnenberg, M. Hada, M. Ehara, K. Toyota, R. Fukuda, J. Hasegawa, M. Ishida, T. Y. Nakajima, O. Honda, H. Kitao, T. Nakai, T. Vreven, J. A. Montgomery Jr, J. E. Peralta, F. Ogliaro, M. Bearpark, J. J. Heyd, E. Brothers, K. N. Kudin, V. N. Staroverov, T. Keith, R. Kobayashi, J. Normand, K. Raghavachari, A. Rendell, J. C. Burant, S. S. Iyengar, J. Tomasi, M. Cossi, N. Rega, J. M. Millam, M. Klene, J. E. Knox, J. B. Cross, V. Bakken, C. Adamo, J. Jaramillo, R. Gomperts, R. E. Stratmann, O. Yazyev, A. J. Austin, R. Cammi, C. Pomelli, J. W. Ochterski, R. L. Martin, K. Morokuma, V. G. Zakrzewski, G. A. Voth, P. Salvador, J. J. Dannenberg, S. Dapprich, A. D. Daniels, O. Farkas, J. B. Foresman, J. V. Ortiz, J. Cioslowski, D. J. Fox, *Gaussian 09, Revision C.01*, Gaussian, Inc., Wallingford CT, 2010.

22 T. Bruhn, A. Schaumlöffel, Y. Hemberger and G. Bringmann, *Chirality*, 2013, **25**, 243.

23 H. J. Zhu, Y. M. Yan, Z. C. Tu, J. F. Luo, R. Liang, T. H. Yang, Y. X. Cheng and S. M. Wang, *Fitoterapia*, 2016, **114**, 163.